INORGANIC CHEMISTRY FRONTIERS

RESEARCH ARTICLE

View Article Online
View Journal

Cite this: DOI: 10.1039/d6qi00380j

Ethylene carbonate splitting and Claisen-type self-addition of γ-butyrolactone promoted by an oxygen-bridged Ga/P FLP

Julian Buth,[a] Beate Neumann,[a] Jan-Hendrik Lamm,[a] Hans-Georg Stammler,[a] Yury V. Vishnevskiy [a,b] and Norbert W. Mitzel *[a]

The versatile reactivity of the geminal oxygen-bridged frustrated Lewis pair (FLP) $Bis_2Ga–O–P^tBu_2$ (Bis = $CH(SiMe_3)_2$; **GaOP**) is presented towards a series of C=O double bonds, strained oxygen-containing rings, alkynes plus alkenes and a C–Cl bond. By adding benzaldehyde, cyclopentanone (CP), γ-butyrolactone (GBL) or ethylene carbonate (EC), classical 1,2-adducts are formed. The reversibility of the **GaOP**·EC adduct stands out, enabling a splitting of EC after several days or when heated to 70 °C, resulting in FLP adducts of CO_2 and ethylene oxide (EO). The latter consists of a six-membered ring and is obtained *via* a ring-opening reaction, as verified by a further reaction involving the similar propylene oxide (PO). The **GaOP**·GBL adduct is further converted, with two adduct molecules combining into a 2 : 1 FLP adduct in a Claisen-type addition and ring-opening. Tests towards various acetylene containing species revealed that the ratio of deprotonation to ring-closure product can be adjusted. While PhC≡CH is almost exclusively bound as the deprotonation product, for Me_3SiC≡CH, the ring-closure product also forms. In the reaction with benzyl chloride, $Bis_2(Cl)Ga–O–P(Bn)^tBu_2$ is formed by a C–Cl bond activation.

Received 25th February 2026,
Accepted 16th April 2026

DOI: 10.1039/d6qi00380j

rsc.li/frontiers-inorganic

Introduction

Understanding the activation and transformation steps of small molecules is of crucial importance for many chemical applications. With the concept of frustrated Lewis pairs (FLPs), D. W. Stephan introduced a way to polarise substrates through the simultaneous action of Lewis acid (LA) and Lewis base (LB) functions.[1] Over the last two decades, this field of research has generated enormous interest, particularly within main-group chemistry and in the pursuit of transition metal-free catalysis.[2–5]

While many transition-metal-based systems boast catalysts for a variety of transformations,[6–13] the investigations of main-group-based FLP-mediated conversions have focused primarily on hydrogenation reactions, C–C couplings and CO_2 reductions.[14–19] Although FLPs are capable of activating many types of small molecules,[20–25] the majority form irreversible adducts, making the development of catalytic reactions difficult. Only a few undergo further transformation due to a conditional reversibility, which is essential for the broader application of FLPs as catalysts.[26,27]

Multiple reactivity studies have shed light on the following adjustment screws for tuning intramolecular FLP reactivity: the combination of LA and LB elements, their respective substituents and the linker unit. The literature predominantly features boron-containing FLP systems that have to bear strongly electron-withdrawing groups in order to be reactive.[28] Such groups are unnecessary for the heavier homologue aluminium, which is inherently more Lewis acidic.[29] However, its strong oxophilicity is a major drawback, particularly when it comes to the release of a transformed product that contains oxygen atoms.

Instead, the group 13 element gallium has a similar Lewis acidity level but prefers softer Lewis bases according to the concept of hard and soft acids and bases (HSAB) by R. G. Pearson.[30,31] W. Uhl *et al.* took advantage of this tendency with the benzylidene-bridged E/P FLPs (E = Al and Ga) in a reaction involving carbon dioxide: the aluminium system irreversibly captures CO_2, while the gallium analogue binds it reversibly.[29,32]

Similarly, adjusting the linker unit, Y. Wang *et al.* have shown the reversibility of a CO_2 adduct with an oxygen-bridged B/P FLP.[33] Reducing the Lewis acidity using donating atoms like oxygen affects the reactivity. Recently, we demonstrated how to tune FLPs for specific reactivities with four chalcogen-

[a]*Lehrstuhl für Anorganische Chemie und Strukturchemie, Centrum für Molekulare Materialen CM2, Fakultät für Chemie, Universität Bielefeld, Universitätsstraße 25, Bielefeld 33615, Germany. E-mail: mitzel@uni-bielefeld.de*
[b]*Department of Chemistry, M. V. Lomonosov Moscow State University, Leninskie Gory 1–3, Moscow 119991, Russia*

bridged systems $Bis_2E–X–P^tBu_2$ (Bis = $CH(SiMe_3)_2$, E = Al and Ga, X = O and S).[34]

As $Bis_2Al–O–P^tBu_2$ (**AlOP**) imposes with H_2 and CO_2 activation, resulting in a reduction of carbon dioxide to the formate stage,[35] $Bis_2Ga–O–P^tBu_2$ (**GaOP**) forms an unusual temperature-dependent H_2 equilibrium by cleavage into Bis_2GaH and $^tBu_2P(O)H$.[36] In particular, this difference in oxophilicity prompted us to test reactivity towards molecules with C═O double bonds and small rings containing oxygen atoms.

In this work, we show impressive reactivities of $Bis_2Ga–O–P^tBu_2$: the cleavage of ethylene carbonate (EC) to ethylene oxide (EO) and CO_2, a Claisen addition of γ-butyrolactone (GBL), the ring opening of propylene oxide (PO) and deprotonation *versus* ring formation of phenyl- and trimethylsilylacetylene plus C–Cl bond activation of benzyl chloride.

Results and discussion

We probed the reactivity of the FLP $Bis_2Ga–O–P^tBu_2$ (**GaOP**) with a series of molecules containing C═O double bonds: benzil, benzophenone, benzaldehyde, cyclopentanone (CP), γ-butyrolactone (GBL) and ethylene carbonate (EC). Unlike the **AlOP** system, which forms a stable 1,2-addition product with benzil, the reaction of the **GaOP** system and benzil ends up in an unselective decomposition. As no reaction was observed with benzophenone, benzaldehyde with a less sterically demanding carbonyl unit was tested, affording the 1,2-adduct **1** (Scheme 1).

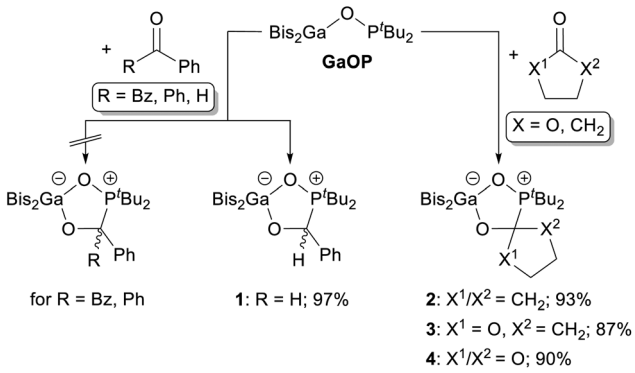

Scheme 1 Reactions of **GaOP** with benzaldehyde, cyclopentanone (CP), γ-butyrolactone (GBL) and ethylene carbonate (EC) to five-membered ring adducts **1–4**. Tests with benzil and benzophenone show decomposition or no reaction.

In the ^1H NMR spectrum, the resonances of the Bis and *tert*-butyl groups are split due to the implemented stereocentre. The chemical shifts of the methine protons at the gallium atom with −0.26 and −0.48 ppm indicate a tetra-coordination. The aldehyde proton resonance at 5.85 ppm is significantly shifted towards higher field compared to "free" benzaldehyde (9.64 ppm). The presence of a five-membered ring is confirmed by $^{13}C\{^1H\}$ NMR spectroscopy with the carbon stereocentre leading to a doublet at 75.5 ppm ($^1J_{P,C}$ = 40.4 Hz) and by $^{31}P\{^1H\}$ NMR with a signal at 70.9 ppm.

Tests towards CP, GBL and EC result in similar adducts **2–4** with five-membered ring motifs (Scheme 1). In all cases, the ^1H NMR signals of the adducts are broadened, indicating weak and potentially reversible adduct formation. In particular, the signals of the CH_2 groups show poor resolution and are low field-shifted in relation to their resonances in the free substrates.

The ^1H NMR shifts of the methine protons range from −0.20 to −0.62 ppm, characteristic of quadruple coordinated gallium atoms (Table 1). Likewise, the $^{13}C\{^1H\}$ and $^{31}P\{^1H\}$ NMR shifts as well as the $^1J_{P,C}$ coupling constants are consistent with normal 1,2-addition adducts.

Further confirmation was provided by elemental analysis and the determination of the molecular structures in the crystalline state, which verified the proposed connectivity for **1**, **2** and **3** (Fig. 1). Despite numerous crystallizations attempts, the ethylene carbonate adduct **4** could only be obtained in a resin-like form.

A comparison of the molecular structures shows similar five-membered rings: the Ga(1)–O(1)–P(1) angles (115.2(2)–115.5(1)°) and the Ga(1)···P(1) distances (2.986(1)–2.990(1) Å) are identical. The gallium atoms are, as expected, in distorted tetrahedral environments, with the O(1)–Ga(1)–O(2) angles ranging from 86.4(4) to 87.0(1)°. Only the O(2)–C(23) bond length varies significantly with 1.44(2) (for **1**), 1.404(2) (for **2**) and 1.360(1) Å (for **3**). However, these values are higher than those of the carbon dioxide adduct (**6**: 1.285(3) Å), evidencing an oxygen–carbon single bond.

Strikingly, the 1,2-addition adducts **3** and **4** undergo further conversions in solution within two days at ambient temperature (partially) or when heated to 70 °C for six hours (fully). The GBL adduct **3** is subject to a rearrangement, forming the adduct type **5** in a Claisen addition and ring-opening reaction (Scheme 2). In this reaction, two molecules of the adduct **3** react to a Claisen addition product, which then forms the α,β-unsaturated ketone resulting from a ring-opening. This

Table 1 ^1H, $^{13}C\{^1H\}$ and $^{31}P\{^1H\}$ NMR spectroscopic data of **1**, **2**, **3**, **4**, **7** and **8**

Compound	No.	$\delta(^1H)$ (GaC**H**)/ppm	$\delta(^1H)$ (^{t}Bu)/ppm	$\delta(^{13}C\{^1H\})$ (P**C**X_3)/ppm	$\delta(^{31}P\{^1H\})$/ppm
GaOP·PhCHO	**1**	−0.48, −0.26	0.84/1.15 ($^3J_{P,H}$ = 13.4/13.3 Hz)	75.5 ($^1J_{P,C}$ = 40.4 Hz)	70.9
GaOP·CP	**2**	−0.62, −0.39	0.99/1.11 ($^3J_{P,H}$ = 13.0/13.3 Hz)	87.0 ($^1J_{P,C}$ = 40.0 Hz)	77.2
GaOP·GBL	**3**	−0.38, −0.20 br.	1.10 br.	109.9 ($^1J_{P,C}$ = 73.2 Hz)	74.1
GaOP·EC	**4**	−0.30 br.	1.19 br.	122.7 ($^1J_{P,C}$ = 120.4 Hz)	70.6
GaOP·EO	**7**	−0.40 br.	0.87 ($^3J_{P,H}$ = 14.0 Hz)	23.7 ($^1J_{P,C}$ = 54.5 Hz)	75.1
GaOP·PO	**8**	−0.49, −0.39	0.85/0.90 ($^3J_{P,H}$ = 13.9/14.0 Hz)	30.0 ($^1J_{P,C}$ = 54.5 Hz)	73.0

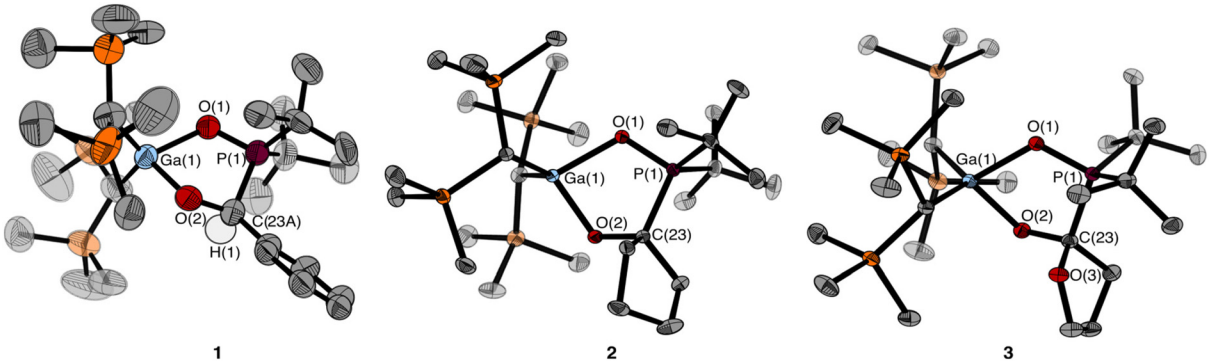

Fig. 1 Molecular structures of **1**, **2** and **3** in the solid state. Hydrogen atoms (except H(1) in **1**) and minor occupied disordered parts are omitted for clarity. Ellipsoids are set at the 50% probability level. Selected distances, bond lengths [Å] and angles [°]: **1**: Ga(1)···P(1) 2.989(1), Ga(1)–O(1) 2.004(2), Ga(1)–O(2A) 1.834(13), O(1)–P(1) 1.524(2), P(1)–C(23A) 1.891(16), O(2)–C(23) 1.44(2); Ga(1)–O(1)–P(1) 115.2(2), C(1A)–Ga(1)–C(8A) 126.9(8), O(1)–Ga(1)–O(2A) 86.4(4), O(2A)–Ga(1)–P(1)–C(23A) 25.0(9); **2**: Ga(1)···P(1) 2.990(1), Ga(1)–O(1) 1.986(1), Ga(1)–O(2) 1.894(1), O(1)–P(1) 1.538(1), P(1)–C(23) 1.897(2), O(2)–C(23) 1.404(2); Ga(1)–O(1)–P(1) 115.5(1), C(1)–Ga(1)–C(8) 119.1(1), O(1)–Ga(1)–O(2) 87.0(1), O(2)–Ga(1)–P(1)–C(23) 18.9(1); **3**: Ga(1)···P(1) 2.986(1), Ga(1)–O(1) 1.993(1), Ga(1)–O(2) 1.907(1), O(1)–P(1) 1.533(1), P(1)–C(23) 1.906(1), O(2)–C(23) 1.360(1); Ga(1)–O(1)–P(1) 115.2(1), C(1)–Ga(1)–C(8) 122.4(1), O(1)–Ga(1)–O(2) 86.9(1), O(2)–Ga(1)–P(1)–C(23) 18.4(1).

molecule is bound to two FLP units. The reaction to **5** is presumably triggered by the deprotonation of the α-proton, resulting in the formation of the P–H unit (Scheme 2 or SI Scheme S1).

Multinuclear NMR spectroscopy analysis approves the formation of **5**. The ^{31}P NMR spectrum shows a doublet of multiplets at 63.2 ppm ($^{1}J_{P,H}$ = 422.9 Hz), confirming the generation of phosphane oxide. The broadened signal indicates its interaction with the Lewis acid moiety. The ^{1}H NMR shifts of the methine protons at −0.30 and −0.48 ppm verify tetra-coordinated gallium atoms and suggest the presence of two different Bis_2Ga-groups, which are also confirmed by ^{29}Si NMR spectroscopy. The framework of the Claisen added and ring-opened product **5** is identified by ^{1}H and $^{13}C\{^{1}H\}$ NMR spectroscopy, with five CH_2 units observable in the ^{13}C DEPT-135 NMR spectrum. The remaining quaternary carbon atoms show shifts of 188.0, 178.7 and 90.7 ppm, respectively. The ^{1}H–^{1}H COSY NMR spectrum validates the correlation of the methylene protons at 3.68 and 2.49 ppm and of those at 4.07, 2.49 and 2.10 ppm. All these assignments are consistent within the corresponding 2D NMR spectra (^{1}H–^{13}C HSQC and HMBC). As for the 1,2-adduct **4**, multiple attempts to crystallize **5** failed and only yielded resin-like residues.

A different transformation is observed for **4**. The added ethylene carbonate (EC) is cleaved, resulting in the formation of the FLP adducts of carbon dioxide (**6**) and of ethylene oxide (EO) (**7**) accompanied by the release of half an equivalent of EC (Scheme 2). This observation lends support to the assumed reversible nature of the adduct formation with EC.

There are two main pathways for the splitting of EC (see SI Scheme S2): the activation of the carbonyl unit followed by ring-opening (path A) or ring-opening, where the carbonate

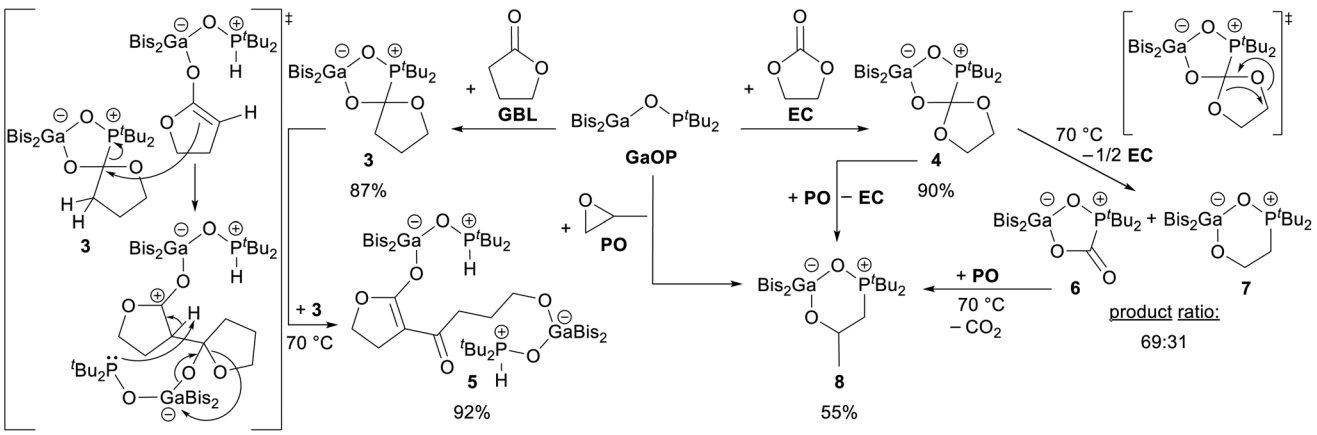

Scheme 2 The 1,2-adduct **3** is further converted in a Claisen-type addition, forming a 2 : 1 FLP Claisen addition adduct with subsequent ring-opening *via* the proposed mechanism and structure **5** (left). Heating **4** to 70 °C results in the splitting of EC, leading to the FLP CO_2 and EO adducts (**6**/**7**) and one half of an equivalent of EC (right). In a ring-opening reaction, propylene oxide forms a six-membered ring adduct **8**. Also exchange reactions of **4** and **6** with propylene oxide (PO) result in adduct **8**.

unit remains intact followed by an extrusion (retro-insertion) of CO_2 leading to the EO adduct **7** (path B). Both pathways have been reported in the literature,[37,38] but the experimental outcome (formation of more CO_2 adduct **6**) matches only path A, as **7** is stable in the presence of CO_2.

In the ^{1}H NMR spectrum one set of signals corresponds to the literature values of **6**.[34] Characteristic of the EO adduct **7** is the doublet of triplets of the oxygen-bound CH_2 group at 4.10 ppm ($^3J_{P,H}$ = 18.5 Hz, $^3J_{H,H}$ = 5.6 Hz). Due to overlapping resonances, it was not possible to localise a resonance for the second CH_2 unit exactly in the ^{1}H NMR spectrum, even when using 2D NMR. In contrast, the $^{13}C\{^1H\}$ NMR spectrum contains a resonance in this regard as a doublet at 23.7 ppm ($^1J_{P,C}$ = 54.5 Hz).

To further verify the formation of a six-membered ring, we reacted **GaOP** with the similar propylene oxide (PO). In a ring-opening reaction the adduct **8** was formed. Both **7** and **8** have comparable chemical shifts. For example, the $^{31}P\{^1H\}$ NMR shifts differ slightly (**7**: 75.1 ppm; **8**: 73.0 ppm). In the $^{13}C\{^1H\}$ NMR spectrum the carbon atom attached to the oxygen atom is detected at 60.5 (**7**) and 65.6 ppm (**8**), respectively. The propylene unit of **8** induces signals at 4.35, 1.63, 1.36 and 1.32 ppm in the ^{1}H NMR spectrum, which are similar to those of **7**. Due to the diastereotopic nature of the P–CH_2 protons, both resonances are split into doublets of multiplets with a characteristic $^3J_{P,H}$ coupling constant of 14.8 Hz (see SI Fig. S38).

Crystal structure determinations of both the EO and PO adducts **7** and **8**, confirm the six-membered ring motif (Fig. 2). Since they differ only by an exocyclic methyl group, the structural parameters are nearly the same. The Ga(1)···P(1) distances of 3.191–3.198(1) Å are longer than in free FLP **GaOP** (3.082(1) Å).[36] The Ga(1)–O(1)–P(1) angles in **7** (129.1(1)°) or **8** (129.3(1)°) are slightly wider than that in **GaOP** of 126.2(1)°.

In an NMR spectroscopic study, we tested the exchange reaction of the ethylene carbonate adduct **4** and the CO_2 adduct **6** with an excess of propylene oxide (PO). When **4** is reacted with PO, the formation of adduct **8** and free EC is observed at ambient temperatures. For **6**, heating to 70 °C is necessary to exchange the carbon dioxide with PO. These findings gave further insights and strengthened the proposed mechanism (path A) of the ethylene carbonate splitting (see SI Scheme S2).

Relating to previous investigations of slightly polarized alkynes with the **AlOP** system,[39] we tested the reactivity of phenyl- and trimethylsilylacetylene with the **GaOP** FLP. Interestingly, there is a clear difference in the product ratio of deprotonation *vs.* ring-closure. Whereas deprotonation predominates in the case of phenylacetylene (>96%), and crystallization gave the deprotonation product **9a** in pure form, only mixtures with deprotonation/ring-closure ratios of approximately 2 : 1 (**10a** : **10b**) were obtained for trimethylsilylacetylene (Scheme 3).

Heating the reaction to 70 °C for 24 h did not result in formation of the ring-closure products **9b** and **10b**. The same behaviour, along with a similar deprotonation/ring-closure ratio, was previously observed for **AlOP**·PhC≡CH (85 : 15).[39] Although the experimental outcome is consistent, quantum chemical calculations suggest that the ring-closure products **9b**/**10b** are thermodynamically favoured (see SI). To explain these contradictions, we assume that the deprotonation products **9a**/**10a** are kinetically preferred and the activation barriers of these meta-stable states to the ring-closure products **9b**/**10b** are too high. Furthermore, a partial separation of **9a** and **10a** into di-*tert*-butylphosphane oxide and $Bis_2GaC{\equiv}CR$ (R = Ph and $SiMe_3$) at higher temperatures, as we reported it for the H_2 adduct of the **GaOP** system,[36] would prevent a rearrangement to ring-closure.

While the ring-closure product **10b** was identified by ^{1}H NMR spectroscopy by its characteristic doublet at 9.25 ppm ($^3J_{P,H}$ = 56.0 Hz), the deprotonation product **10a** has a typical doublet at 5.97 ppm with a $^1J_{P,H}$ coupling constant of 442.2 Hz. The ^{31}P NMR spectrum displays a doublet of multiplets with the same large coupling constant at 66.9 ppm (**10a**) and a single multiplet at 84.8 ppm (**10b**), confirming the identity of these two species. However, the ^{1}H NMR integral ratios of the

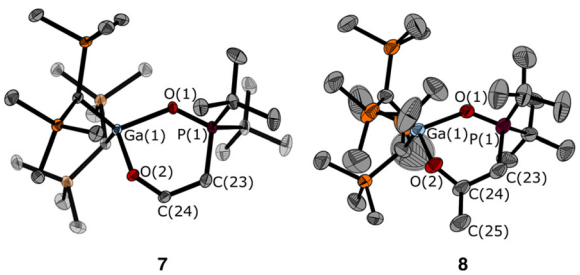

Fig. 2 Molecular structures of **7** and **8** in the solid state. Hydrogen atoms and minor occupied parts are omitted for clarity. Ellipsoids are set at the 50% probability level. Selected distances, bond lengths [Å] and angles [°]: **7**: Ga(1)···P(1) 3.198(1), Ga(1)–O(1) 2.007(1), Ga(1)–O(2) 1.866 (1), O(1)–P(1) 1.527(1), P(1)–C(23) 1.826(1), C(23)–C(24) 1.535(2), O(2)–C (24) 1.401(1); Ga(1)–O(1)–P(1) 129.1(1), O(1)–Ga(1)–O(2) 92.3(1), O(2)–Ga (1)–P(1)–C(23) 15.2(1); **8**: Ga(1)···P(1) 3.191(1), Ga(1)–O(1) 2.001(2), Ga(1)–O(2) 1.854(3), O(1)–P(1) 1.523(2), P(1)–C(23) 1.847(4), C(23)–C(24) 1.520 (6), O(2)–C(24) 1.393(5); Ga(1)–O(1)–P(1) 129.3(1), O(1)–Ga(1)–O(2) 93.1 (1), O(2)–Ga(1)–P(1)–C(23) 14.3(3).

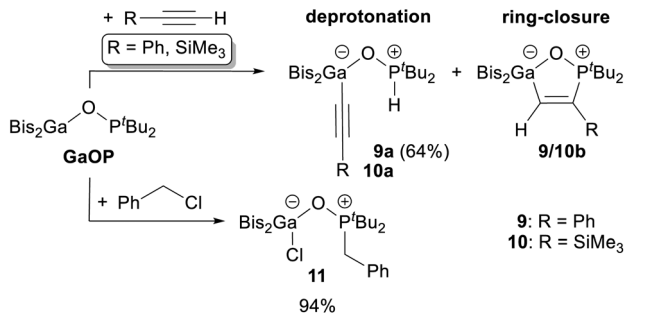

Scheme 3 Reactions of **GaOP** with phenylacetylene and trimethylsilylacetylene result in deprotonation (**9a**/**10a**) or ring-closure (**9b**/**10b**) products. Using benzyl chloride leads to $Bis_2(Cl)Ga{-}O{-}P(H)^tBu_2$ (**11**).

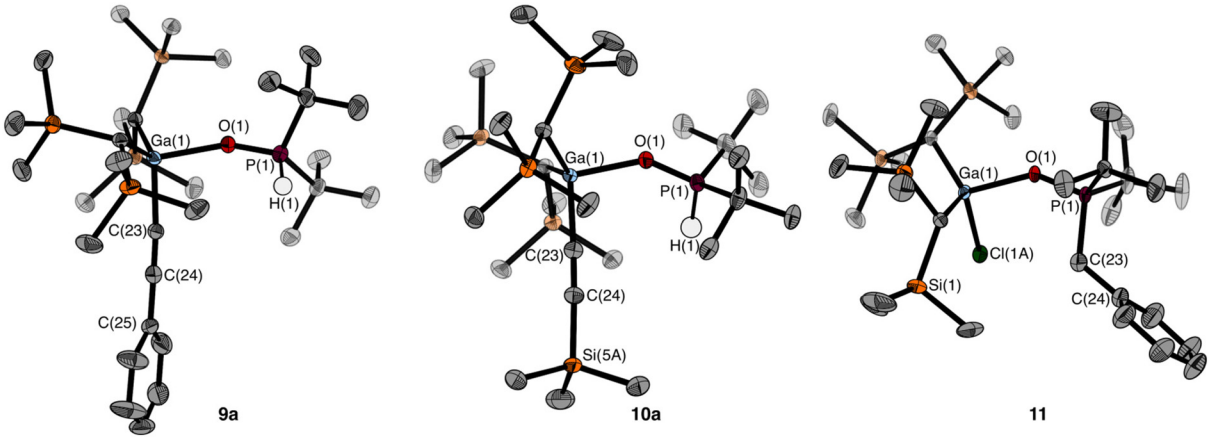

Fig. 3 Molecular structures of **9a**, **10a** and **11** in the solid state. Hydrogen atoms except H(1) and minor occupied disordered parts are omitted for clarity. Ellipsoids are set at the 50% probability level. Selected distances, bond lengths [Å] and angles [°]: **9a**: Ga(1)···P(1) 3.469(1), Ga(1)–O(1) 2.037(1), O(1)–P(1) 1.512(1), Ga(1)–C(23) 2.004(1), C(23)–C(24) 1.187(2); Ga(1)–O(1)–P(1) 155.3(1), C(1)–Ga(1)–C(8) 117.9(1), C(23)–Ga(1)–P(1)–H(1) 57.0(8); **10a**: Ga(1)···P(1) 3.338(1), Ga(1)–O(1) 2.008(1), O(1)–P(1) 1.514(1), Ga(1)–C(23) 1.978(2), C(23)–C(24) 1.206(2); Ga(1)–O(1)–P(1) 142.4(1), C(1)–Ga(1)–C(8) 121.6(1), C(23)–Ga(1)–P(1)–H(1) 41.1(9). **11**: Ga(1)···P(1) 3.371(1), Ga(1)–O(1) 2.014(2), O(1)–P(1) 1.528(2), Ga(1)–Cl(1A) 2.257(3), P(1)–C(23) 1.827(3); Ga(1)–O(1)–P(1) 143.8(1), C(1)–Ga(1)–C(8) 122.8(1), Cl(1A)–Ga(1)–P(1)–C(23) 45.9(1).

deprotonation product **10b** do not match exactly; there is a surplus of phosphane oxide present. Besides hydrolysis, the aforementioned partial separation into the phosphane oxide species and $Bis_2GaC{\equiv}CSiMe_3$ is probably another plausible explanation for these mismatching integral ratios. The excess of phosphane oxide undergoes a dynamic exchange with the deprotonation product **10a**, meaning no "free" phosphane oxide being detected in the ^{31}P NMR spectrum. Elemental analyses confirm this hypothesis and the compositions of **9** and **10**.

We were able to determine the solid-state molecule structures of the deprotonation products **9a** and **10a** (Fig. 3). Contrary to the structure of **AlOP**·PhC≡CH in both forms,[39] and although the formation of the ring-closure product **10b** is evident by NMR spectroscopy, the crystalline sample showed no evidence for different types of crystals. The determined bond lengths of C(23)–C(24) in the deprotonation products fall over the expected range for triple bonds (**9a**: 1.186(3) Å; **10a**: 1.206(2) Å). The angles ∠(Ga–C≡C) (**9a**: 175.3(2)°; **10a**: 177.5 (2)°) and ∠(C≡C–R) (**9a**: 178.5(2)°; **10a**: 178.0(2)°) in the acetylide units are similar, nearly matching an idealized bond angle of 180°. In contrast, both structures differ in their Ga(1)–O(1)–P(1) angles (**9a**: 155.3(1)°; **10a**: 142.4(1)°) and their torsion angles τ(C(23)–Ga(1)–P(1)–H(1)) with 57.0(8)° for **9a** and 41.1 (9)° for **10a**. These values for the heavier gallium homologue **9a** are significantly smaller than those of its aluminium analogue **AlOP**·PhC≡CH (168.8(2)°; 95.9(5)°).[39]

Activation attempts with the non-polar diphenylacetylene and the alkene species styrene, stilbene, 1,2-diphenylethene and 1-phenyl-1-(trimethylsiloxyl)ethylene remained unsuccessful. However, we demonstrated the versatility of the **GaOP** FLP by reacting it with benzyl chloride. After heating to 70 °C, the adduct $Bis_2(Cl)Ga–O–P(Bn)^tBu_2$ (**11**) was isolated and fully characterized by means of NMR spectroscopy, elemental analysis and single crystal X-ray diffraction experiments (Fig. 3). Cleavage of the C–Cl bond resulted in the chloride ion bound to the Lewis acidic gallium and a benzyl group attached to the phosphorus atom.

In the ^1H NMR spectrum the formation of **11** is proven by a doublet of the CH_2 group at 3.40 ppm ($^3J_{P,H}$ = 14.0 Hz). The broad methine proton singlet at −0.06 ppm verifies the tetracoordinated gallium atom. Besides the signal at 63.6 ppm, another species containing a P–H unit was detected by a doublet ^{31}P NMR resonance at 69.7 ppm ($^1J_{P,H}$ = 451.5 Hz). This minor impurity was identified as the formal hydrogen chloride adduct $Bis_2(Cl)Ga–O–P(H)^tBu_2$, likely originating from the partial hydrolysis of benzyl chloride. The chemical shifts are comparable with those of the recently published HBr adduct, **GaOP**·HBr.[36]

The molecular structure of **11** shows a tetrahedral environment at the gallium atom and the Ga(1)–Cl(1A) bond length of 2.257(3) Å is slightly longer than in the free Bis_2GaCl (2.193(1) Å).[40] Compared with **GaOP**·HBr, the Ga(1)–O(1)–P(1) angles are almost identical (**GaOP**·HBr: 143.1(1)°; **11**: 143.8(1)°). As the value of τ(C(23)–Ga(1)–P(1)–H(1)) = 45.9(1)° indicates, the chloride ion and benzyl group are twisted, in a similar manner to the proton and acetylide unit in the deprotonation adducts **9a** and **10a**.

Conclusions

$Bis_2Ga–O–P^tBu_2$ (**GaOP**) exhibits a remarkably broad and tuneable reactivity profile towards a wide variety of substrates, ranging from carbonyl compounds to strained oxygen heterocycles, alkynes and polar σ-bonds. In classical 1,2-additions to the C=O double bond of benzaldehyde, cyclopentanone (CP), γ-butyrolactone (GBL) and ethylene carbonate (EC), FLP

adducts with five-membered rings are observed. Beyond simple adduct formation, the system reveals unexpected secondary transformations such as the Claisen-type reaction of two GBL adducts and subsequent trapping of the resulting product as a 2 : 1 FLP adduct. The reversible activation of EC is particularly notable, as it enables a fragmentation into CO_2 and ethylene oxide (EO), both of which were detected as the corresponding FLP adducts. This ring-opening reaction to a six-membered ring was proven using propylene oxide (PO), which results in the formation of a similar adduct. Reactions involving phenyl- and trimethylsilylacetylene further demonstrate that subtle changes in the substrate structure allow deprotonation and ring-closure to be deliberately steered, providing rare insight into selectivity control in FLP chemistry. Activating the C–Cl bond in benzyl chloride broadens the scope of activation to include polar σ-bonds. Taken together, these findings establish the **GaOP** system as a highly versatile and adaptable FLP, capable of reversible activation, bond cleavage and multistep substrate transformation.

Experimental section

General methods

All reactions and manipulations with air and moisture sensitive compounds were carried out under conventional Schlenk techniques or in a glove box using argon as an inert gas. Volatile compounds were handled in a vacuum line. The solvents *n*-hexane, toluene, toluene-d_8 and benzene-d_6 were dried over a Na/K alloy, distilled and degassed prior to use. $Bis_2Ga–O–P^tBu_2$ (**GaOP**) was prepared according to a literature procedure.[36] Benzaldehyde, cyclopentanone (CP), γ-butyrolactone (GBL), propylene oxide (PO), phenylacetylene, trimethylsilyl acetylene and benzyl chloride were degassed, dried over molecular sieves (4 Å) and distilled prior to use. Ethylene carbonate (EC) was used without further purification. NMR spectra were recorded using a Bruker Avance III 500, Avance III 500 HD, Ascend 500 neo2K or Ascend 500 neo3K spectrometer at ambient temperature unless otherwise stated. Chemical shifts were referenced to the residual proton or carbon signal of the solvent (benzene-d_6: ^{1}H: 7.16 ppm, ^{13}C: 128.1 ppm; toluene-d_8: ^{1}H: 2.09 ppm) or externally (^{29}Si: $SiMe_4$, ^{31}P: 85% H_3PO_4 in H_2O). Elemental analyses were carried out using a HEKATECH EURO elemental analyzer.

Synthetic procedure

$Bis_2Ga–O–P^tBu_2$ (**GaOP**) was dissolved in toluene (2 mL), the substrate was added and the reaction was stirred for 24 h at room temperature, unless otherwise stated. All volatiles were removed under reduced pressure and the residue was dried *in vacuo*.

$Bis_2Ga–O–P^tBu_2$·PhCHO (1). Using benzaldehyde (5 μL, 4.8 mg, 45 μmol, 1.2 equiv.) and after an additional washing step with *n*-hexane, **1** was obtained as a colourless solid (24 mg, 37 μmol, 97%). ^{1}H NMR (500 MHz, C_6D_6): δ [ppm] = −0.48 (s, 1H, GaC**H**), −0.26 (s, 1H, GaC**H**), 0.36–0.58 (m, 36H, Si(C**H**$_3$)$_3$), 0.84 (d, $^3J_{P,H}$ = 13.4 Hz, 9H, C(C**H**$_3$)$_3$), 1.15 (d, $^3J_{P,H}$ = 13.3 Hz, 9H, C(C**H**$_3$)$_3$), 5.85 (s, C**H**O), 7.02 (t, $^3J_{H,H}$ = 7.2 Hz, 1H, *para*-**H**), 7.14 (t, $^3J_{H,H}$ = 7.3 Hz, 2H, *meta*-**H**), 7.72 (d, $^3J_{H,H}$ = 7.6 Hz, 2H, *ortho*-**H**). ^{13}C{^{1}H} NMR (126 MHz, C_6D_6): δ [ppm] = 3.9 (s, Si(**C**H$_3$)$_3$), 4.6(s, Si(**C**H$_3$)$_3$), 4.6 (s, Si(**C**H$_3$)$_3$), 4.8 (s, Si(**C**H$_3$)$_3$), 6.6 (s, Ga**C**H), 27.1 (s, C(**C**H$_3$)$_3$), 28.2 (s, C(**C**H$_3$)$_3$), 35.3 (s, **C**(CH$_3$)$_3$), 37.0 (s, **C**(CH$_3$)$_3$), 75.5 (d, $^1J_{P,C}$ = 40.4 Hz, **C**HO), 126.3 (s, *ortho*-**C**), 127.2 (s, *para*-**C**), 128.3 (s, *meta*-**C**), 141.6 (s, *ipso*-**C**). ^{29}Si{^{1}H} NMR (99 MHz, C_6D_6): δ [ppm] = −1.1 (s). ^{31}P{^{1}H} NMR (202 MHz, C_6D_6): δ [ppm] = 70.9 (s). Elemental analysis calcd (%) for $C_{29}H_{62}GaO_2PSi_4$ (M_r = 655.85): C 53.11, H 9.53; found C 53.57, H 9.54.

$Bis_2Ga–O–P^tBu_2$·CP (2). Using cyclopentanone (10 μL, 9.5 mg, 113 μmol, 1.2 equiv.) and after an additional washing step with *n*-hexane, **2** was obtained as a colourless solid (58 mg, 91 μmol, 93%). ^{1}H NMR (500 MHz, C_6D_6): δ [ppm] = −0.62 (s, 1H, GaC**H**), −0.39 (s, 1H, GaC**H**), 0.42–0.50 (s, 36H, Si(C**H**$_3$)$_3$), 0.99 (d, $^3J_{P,H}$ = 13.0 Hz, 9H, C(C**H**$_3$)$_3$), 1.11 (d, $^3J_{P,H}$ = 13.3 Hz, 9H, C(C**H**$_3$)$_3$), 1.48(m, 2H, C**H**$_2$), 1.66 (m, 2H, C**H**$_2$), 2.03 (m, 4H, C**H**$_2$). ^{13}C{^{1}H} NMR (126 MHz, C_6D_6): δ [ppm] = 5.3 (s, Si(**C**H$_3$)$_3$), 6.8 (s, Ga**C**H), 9.9 (s, Ga**C**H), 23.5 (d, $^2J_{P,C}$ = 11.9 Hz, **C**H$_2$), 23.8 (d, $^2J_{P,C}$ = 12.4 Hz, **C**H$_2$), 28.2 (s, C(**C**H$_3$)$_3$), 28.8 (s, C(**C**H$_3$)$_3$), 35.8 (d, $^1J_{P,C}$ = 41.4 Hz, **C**(CH$_3$)$_3$), 37.5 (d, $^1J_{P,C}$ = 41.8 Hz, **C**(CH$_3$)$_3$), 41.1 (s, **C**H$_2$), 42.5 (s, **C**H$_2$), 87.0 (d, $^1J_{P,C}$ = 40.0 Hz, P**C**O). ^{29}Si{^{1}H} NMR (99 MHz, C_6D_6): δ [ppm] = −1.2 (s). ^{31}P{^{1}H} NMR (202 MHz, C_6D_6): δ [ppm] = 77.2 (s). Elemental analysis calcd (%) for $C_{27}H_{64}GaO_2PSi_4$ (M_r = 633.84): C 51.16, H 10.18; found C 50.78, H 10.14.

$Bis_2Ga–O–P^tBu_2$·GBL (3). Using γ-butyrolactone (10 μL, 11.3 mg, 131 μmol, 1.0 equiv.) and after an additional washing step with *n*-hexane, **3** was obtained as a colourless solid (70 mg, 110 μmol, 87%). ^{1}H NMR (500 MHz, C_6D_6): δ [ppm] = −0.38 (br. s, 1H, GaC**H**), −0.20 (br. s, 1H, GaC**H**), 0.45 (s, 36H, Si(C**H**$_3$)$_3$), 1.10 (m, 18H, C(C**H**$_3$)$_3$), 1.44 (m, 1H, C**H**$_2$), 1.60 (br. m, 1H, C**H**$_2$), 1.93 (br. s, 1H, C**H**$_2$), 2.11 (br. s, 1H, C**H**$_2$), 3.32 (br. s, 1H, C**H**$_2$), 4.00 (br. s, 1H, C**H**$_2$). ^{13}C{^{1}H} NMR (126 MHz, C_6D_6): δ [ppm] = 5.1 (s, Si(**C**H$_3$)$_3$), 9.2 (s, Ga**C**H), 24.7 (s, **C**H$_2$), 27.8 (s, C(**C**H$_3$)$_3$), 35.6 (d, $^1J_{P,C}$ = 47.5 Hz, **C**(CH$_3$)$_3$), 36.4 (d, $^1J_{P,C}$ = 48.5 Hz, **C**(CH$_3$)$_3$), 39.6 (s, **C**H$_2$), 67.1 (s, O**C**H$_2$), 109.9 (d, $^1J_{P,C}$ = 73.2 Hz, P**C**O$_2$). ^{29}Si{^{1}H} NMR (99 MHz, C_6D_6): δ [ppm] = −1.5 (s). ^{31}P{^{1}H} NMR (202 MHz, C_6D_6): δ [ppm] = 74.1 (s). Elemental analysis calcd (%) for $C_{26}H_{62}GaO_3PSi_4$ (M_r = 635.82): C 49.12, H 9.83; found C 48.61, H 10.23.

$Bis_2Ga–O–P^tBu_2$·EC (4). Using ethylene carbonate (9.1 mg, 103 μmol, 1.1 equiv.) and after an additional washing step with *n*-hexane, **4** was obtained in a colourless, resin-like form (52 mg, 82 μmol, 90%). ^{1}H NMR (500 MHz, C_6D_6): δ [ppm] = −0.30 (br. s, 2H, GaC**H**), 0.45 (s, 36H, Si(C**H**$_3$)$_3$), 1.19 (m, 18H, C(C**H**$_3$)$_3$), 3.28 (br. s, 2H, C**H**$_2$), 3.80 (br. s, 2H, C**H**$_2$). ^{13}C{^{1}H} NMR (126 MHz, C_6D_6): δ [ppm] = 4.9 (s, Si(**C**H$_3$)$_3$), 9.0 (s, Ga**C**H), 27.5 (s, C(**C**H$_3$)$_3$), 35.8 (br. m, **C**(CH$_3$)$_3$), 63.4 (s, O**C**H$_2$), 122.7 (d, $^1J_{P,C}$ = 120.4 Hz, P**C**O$_3$). ^{29}Si{^{1}H} NMR (99 MHz, C_6D_6): δ [ppm] = −1.3 (s). ^{31}P{^{1}H} NMR (202 MHz, C_6D_6): δ [ppm] = 70.6 (s). Elemental analysis calcd (%) for $C_{25}H_{60}GaO_4PSi_4$ (M_r = 637.79): C 47.08, H 9.48; found C 46.99, H 9.56.

Claisen addition ring-opening FLP adduct 5. Heating a solution of **GaOP** (55.7 mg, 101 μmol) and GBL (7.9 μL, 8.9 mg, 104 μmol, 1.0 equiv.) in toluene (3 mL) to 70 °C for 6 h, full conversion of the FLP to **5** was observed. After removing all volatiles *in vacuo*, and an additional washing step with *n*-hexane, **5** was obtained in a resin-like form (59.4 mg, 47 μmol, 92%). ^{1}H NMR (500 MHz, C_6D_6): δ [ppm] = −0.48 (s, 2H, GaC**H**), −0.30 (s, 2H, GaC**H**), 0.34 (s, 36H, Si(C**H**$_3$)$_3$), 0.34 (s, 18H, Si(C**H**$_3$)$_3$), 0.36 (s, 18H, Si(C**H**$_3$)$_3$), 0.99 (d, $^{3}J_{P,H}$ = 15.0 Hz, 18H, C(C**H**$_3$)$_3$), 2.10 (tt, J = 11.9, 5.8 Hz, 2H, C**H**), 2.49 (m, 2H, C**H**), 2.49 (t, J = 8.3 Hz, 2H, C**H**), 3.68 (t, J = 8.2 Hz, 2H, C**H**), 4.07 (t, J = 6.0 Hz, 2H, C**H**$_2$). ^{13}C{^{1}H} NMR (126 MHz, C_6D_6): δ [ppm] = 3.9/4.1/4.5 (s, Si(**C**H$_3$)$_3$), 7.5/10.3 (s, Ga**C**H), 25.8 (s, C(**C**H$_3$)$_3$), 26.0 (s, **C**H$_2$), 30.9 (s, **C**H$_2$), 33.6 (d, $^{1}J_{P,C}$ = 59.0 Hz, **C**(CH$_3$)$_3$), 36.1 (s, **C**H$_2$), 65.7 (s, O**C**H$_2$), 67.8 (s, O**C**H$_2$), 90.7 (s, **C**CO$_2$Ga), 178.7 (s, **C**O$_2$Ga), 188.0 (s, **C**=O). ^{29}Si{^{1}H} NMR (99 MHz, C_6D_6): δ [ppm] = −1.4 (s), −0.5 (s), −0.3 (s). ^{31}P{^{1}H} NMR (202 MHz, C_6D_6): δ [ppm] = 63.2 (s).

Bis$_2$Ga–O–P^{t}Bu$_2$·EO (7). After heating a solution of **GaOP** (60.5 mg, 110 μmol) and EC (9.6 mg, 110 μmol, 1.0 equiv.) in toluene (3 mL) to 70 °C for 6 h, full conversion of the FLP to a mixture of Bis$_2$Ga–O–P^{t}Bu$_2$·CO$_2$ (**6**) and **7** was observed. The chemical shifts of **6** are in accordance with the literature values.[34] Crystals of **7**, suitable for X-ray diffraction experiments, were obtained by the slow evaporation of a solution in C_6D_6. ^{1}H NMR (500 MHz, C_6D_6): δ [ppm] = −0.40 (br. s, 2H, GaC**H**), 0.49 (s, 36H, Si(C**H**$_3$)$_3$), 0.87 (d, $^{3}J_{P,H}$ = 14.0 Hz, 18H, C(C**H**$_3$)$_3$), 4.10 (dt, $^{3}J_{P,H}$ = 18.5 Hz, $^{3}J_{H,H}$ = 5.6 Hz, 2H, OC**H**$_2$); due to overlapping resonances, as well in 2D spectra, signals for PC**H**$_2$ could not be localized exactly. ^{13}C{^{1}H} NMR (126 MHz, C_6D_6): δ [ppm] = 5.1 (s, Si(**C**H$_3$)$_3$), 10.5 (s, Ga**C**H), 23.7 (d, $^{1}J_{P,C}$ = 54.5 Hz, P**C**H$_2$), 25.9 (s, C(**C**H$_3$)$_3$), 26.2 (s, C(**C**H$_3$)$_3$), 33.6 (d, $^{1}J_{P,C}$ = 58.9 Hz, **C**(CH$_3$)$_3$), 35.4 (d, $^{1}J_{P,C}$ = 58.3 Hz, **C**(CH$_3$)$_3$), 60.5 (d, $^{2}J_{P,C}$ = 7.6 Hz, O**C**H$_2$). ^{29}Si{^{1}H} NMR (99 MHz, C_6D_6): δ [ppm] = −0.5 (s). ^{31}P{^{1}H} NMR (202 MHz, C_6D_6): δ [ppm] = 75.1 (s).

Bis$_2$Ga–O–P^{t}Bu$_2$·PO (8). Using propylene oxide (10 μL, 8.3 mg, 143 μmol, 1.5 equiv.), the ring-opening adduct **8** crystallized from *n*-hexane at −18 °C, giving colourless needles (32 mg, 53 μmol, 55%). ^{1}H NMR (500 MHz, C_6D_6): δ [ppm] = −0.49 (s, 1H, GaC**H**), −0.39 (s, 1H, GaC**H**), 0.42–0.56 (m, 36H, Si(C**H**$_3$)$_3$), 0.85 (d, $^{3}J_{P,H}$ = 13.9 Hz, 9H, C(C**H**$_3$)$_3$), 0.90 (d, $^{3}J_{P,H}$ = 14.0 Hz, 9H, C(C**H**$_3$)$_3$), 1.32 (ddd, J = 14.8, 3.7, 1.8 Hz, PC**H**$_2$), 1.36 (dd, J = 5.7, 2.7 Hz, C**H**$_3$), 1.63 (ddd, J = 14.8, 10.8, 8.8 Hz, PC**H**$_2$), 4.35 (m, 1H, OC**H**). ^{13}C{^{1}H} NMR (126 MHz, C_6D_6): δ [ppm] = 4.8 (s, overlapped, from ^{1}H–^{13}C HSQC experiment, Ga**C**H), 4.9 (s, Si(**C**H$_3$)$_3$), 5.2 (s, Si(**C**H$_3$)$_3$), 5.6 (s, Si(**C**H$_3$)$_3$), 5.6 (s, overlapped, from ^{1}H–^{13}C HSQC experiment, Ga**C**H), 26.2 (s, C(**C**H$_3$)$_3$), 26.5 (s, C(**C**H$_3$)$_3$), 29.4 (d, $^{3}J_{P,C}$ = 13.6 Hz, **C**H$_3$), 30.0 (d, $^{1}J_{P,C}$ = 54.5 Hz, P**C**H$_2$), 35.1 (d, $^{1}J_{P,C}$ = 57.7 Hz, **C**(CH$_3$)$_3$), 35.7 (d, $^{1}J_{P,C}$ = 59.0 Hz, **C**(CH$_3$)$_3$), 65.6 (d, $^{2}J_{P,C}$ = 5.9 Hz, O**C**H). ^{29}Si{^{1}H} NMR (99 MHz, C_6D_6): δ [ppm] = −1.7 (s), −1.1 (s), −0.7 (s), −0.2 (s). ^{31}P{^{1}H} NMR (202 MHz, C_6D_6): δ [ppm] = 73.0 (s). Elemental analysis calcd (%) for $C_{25}H_{62}GaO_2PSi_4$ (M_r = 607.81): C 49.40, H 10.28; found C 49.14, H 10.53.

Bis$_2$Ga–O–P^{t}Bu$_2$·PhC≡CH (9). Using phenylacetylene (10 μL, 9.3 mg, 91 μmol, 1.0 equiv.) and stirring at 70 °C, **9a** was recrystallized from *n*-hexane at −18 °C, giving colourless needles of the deprotonation product (38 mg, 59 μmol, 64%). ^{1}H NMR (500 MHz, C_6D_6): δ [ppm] = −0.31 (s, 2H, GaC**H**), 0.46 (s, 36H, Si(C**H**$_3$)$_3$), 0.95 (d, $^{3}J_{P,H}$ = 15.7 Hz, 18H, C(C**H**$_3$)$_3$), 5.98 (d, $^{1}J_{P,H}$ = 440.1 Hz, 1H, P**H**), 6.98 (t, $^{3}J_{H,H}$ = 7.4 Hz, 1H, *para*-**H**), 7.05 (t, $^{3}J_{H,H}$ = 7.3 Hz, 2H, *meta*-**H**), 7.62 (d, $^{3}J_{H,H}$ = 7.8 Hz, 2H, *ortho*-**H**). ^{13}C{^{1}H} NMR (126 MHz, C_6D_6): δ [ppm] = 4.6 (s, Si(**C**H$_3$)$_3$), 10.0 (s, Ga**C**H), 26.0 (s, C(**C**H$_3$)$_3$), 33.8 (d, $^{1}J_{P,C}$ = 58.4 Hz, **C**(CH$_3$)$_3$), 109.7 (s, PhC≡**C**Ga), 126.1 (s, Ph**C**≡CGa), 127.6 (s, *para*-**C**), 128.4 (s, *ipso*-**C**), 128.6 (s, *meta*-**C**), 131.6 (s, *ortho*-**C**). ^{29}Si{^{1}H} NMR (99 MHz, C_6D_6): δ [ppm] = −0.9 (s). ^{31}P{^{1}H} NMR (202 MHz, C_6D_6): δ [ppm] = 67.3 (s). Elemental analysis calcd (%) for $C_{30}H_{62}GaOPSi_4$ (M_r = 651.86): C 55.28, H 9.59; found C 54.61, H 9.88.

Bis$_2$Ga–O–P^{t}Bu$_2$·Me$_3$SiC≡CH (10). Using trimethylsilylacetylene (10 μL, 7.1 mg, 72 μmol, 1.0 equiv.), stirring at 70 °C and after an additional washing step with *n*-hexane, **10** was obtained in a colourless resin-like form (41 mg, 63 μmol, 92%). Deprotonation product (**10a**): ^{1}H NMR (500 MHz, C_6D_6): δ [ppm] = −0.50 (s, 2H, GaC**H**), 0.27 (s, 9H, Si(C**H**$_3$)$_3$), 0.46 (s, 36H, CH(Si(C**H**$_3$)$_3$)$_2$), 0.96 (d, $^{3}J_{P,H}$ = 15.6 Hz, 18H, C(C**H**$_3$)$_3$), 5.97 (d, $^{1}J_{P,H}$ = 442.2 Hz, 1H, P**H**). ^{13}C{^{1}H} NMR (126 MHz, C_6D_6): δ [ppm] = 0.3 (s, Si(**C**H$_3$)$_3$), 4.8 (s, Si(**C**H$_3$)$_3$), 8.2 (s, Ga**C**H), 26.2 (s, C(**C**H$_3$)$_3$), 33.8 (d, $^{1}J_{P,C}$ = 58.3 Hz, **C**(CH$_3$)$_3$), 115.7 (s, Me$_3$SiC≡**C**Ga), 134.8 (s, Me$_3$Si**C**≡CGa). ^{29}Si{^{1}H} NMR (99 MHz, C_6D_6): δ [ppm] = −22.9 (s), −0.7 (s). ^{31}P{^{1}H} NMR (202 MHz, C_6D_6): δ [ppm] = 66.9 (s). Elemental analysis calcd (%) for $C_{27}H_{66}GaOPSi_5$ (M_r = 647.95): C 50.05, H 10.27; found C 49.81, H 10.37. Ring-closure product (**10b**): ^{1}H NMR (500 MHz, C_6D_6): δ [ppm] = −0.50 (br. s, 2H, GaC**H**), 0.18 (s, 9H, Si(C**H**$_3$)$_3$), 0.38–0.43 (s, 36H, CH(Si(C**H**$_3$)$_3$)$_2$), 1.02 (d, $^{3}J_{P,H}$ = 14.0 Hz, 18H, C(C**H**$_3$)$_3$), 9.25 (d, $^{3}J_{P,H}$ = 56.0 Hz, 1H, PC**H**). ^{13}C{^{1}H} NMR (126 MHz, C_6D_6): δ [ppm] = 2.0 (s, Si(**C**H$_3$)$_3$), 5.1/5.4 (s, Si(**C**H$_3$)$_3$), 27.5 (s, C(**C**H$_3$)$_3$), 35.1 (d, $^{1}J_{P,C}$ = 56.3 Hz, **C**(CH$_3$)$_3$), 139.9 (d, $^{1}J_{P,C}$ = 41.4 Hz, GaC=**C**P), 206.7 (d, $^{2}J_{P,C}$ = 5.9 Hz, Ga**C**=CP); a signal for Ga**C**H could not be observed. ^{29}Si{^{1}H} NMR (99 MHz, C_6D_6): δ [ppm] = −8.2 (s), −1.6 (s). ^{31}P{^{1}H} NMR (202 MHz, C_6D_6): δ [ppm] = 84.8 (s).

Bis$_2$(Cl)Ga–O–P(Bn)^{t}Bu$_2$ (11). Using benzyl chloride (10 μL, 9.1 mg, 72 μmol, 1.0 equiv.), stirring at 70 °C and after an additional washing step with *n*-hexane, **11** was obtained as a light yellow solid (44 mg, 65 μmol, 94%). ^{1}H NMR (500 MHz, C_6D_6): δ [ppm] = −0.06 (s, 2H, GaC**H**), 0.36 (s, 36H, Si(C**H**$_3$)$_3$), 1.06 (d, $^{3}J_{P,H}$ = 13.6 Hz, 18H, C(C**H**$_3$)$_3$), 3.40 (d, $^{3}J_{P,H}$ = 14.0 Hz, 2H, C**H**$_2$), 7.00 (t, $^{3}J_{H,H}$ = 7.3 Hz, 1H, *para*-**H**), 7.05 (t, $^{3}J_{H,H}$ = 7.6 Hz, 2H, *meta*-**H**), 7.39 (d, $^{3}J_{H,H}$ = 7.9 Hz, 2H, *ortho*-**H**). ^{13}C{^{1}H} NMR (126 MHz, C_6D_6): δ [ppm] = 4.3 (s, Si(**C**H$_3$)$_3$), 15.8 (s, Ga**C**H), 27.5 (s, C(**C**H$_3$)$_3$), 31.2 (d, $^{1}J_{P,C}$ = 48.4 Hz, **C**H$_2$), 36.7 (d, $^{1}J_{P,C}$ = 56.3 Hz, **C**(CH$_3$)$_3$), 127.0 (d, $^{4}J_{P,C}$ = 2.5 Hz, *para*-**C**), 128.7 (s, *meta*-**C**), 130.8 (d, $^{3}J_{P,C}$ = 5.0 Hz, *ortho*-**C**), 134.3 (d, $^{2}J_{P,C}$ = 6.0 Hz, *ipso*-**C**). ^{29}Si{^{1}H} NMR (99 MHz, C_6D_6): δ [ppm] = −1.3 (s). ^{31}P{^{1}H} NMR (202 MHz, C_6D_6): δ [ppm] = 63.6 (s). Elemental analysis calcd (%) for $C_{29}H_{63}GaOPSi_4$ (M_r = 676.31): C 51.50, H 9.39; found C 51.67, H 9.59.

Author contributions

J. Buth: investigation, methodology, validation, visualization, and writing (original draft); B. Neumann, J.-H. Lamm and H.-G. Stammler: investigation (SCXRD); Y. V. Vishnevskiy (quantum chemical calculations) and N. W. Mitzel: funding acquisition, project administration, supervision, writing, reviewing and editing.

Conflicts of interest

There are no conflicts to declare.

Data availability

The data supporting this article have been included as part of the supplementary information (SI). Supplementary information (SI): experimental details, NMR spectra, crystallographic details, quantum chemical calculations (coordinates provided in a separate file), and references. See DOI: **https://doi.org/10.1039/d6qi00380j**.

CCDC 2528994–2529001 (for compounds **1**, **2**, **7**, **8**, **9a**, **10a** and **11**) contain the supplementary crystallographic data for this paper.[41a–h]

Acknowledgements

The authors thank Marco Wißbrock and Dr Andreas Mix for recording NMR spectra, Barbara Teichner for performing elemental analyses and Hannah Koch for providing support with syntheses.

This work was funded by the Deutsche Forschungsgemeinschaft (DFG, German Research Foundation, grant MI 477/44-1, project no. 461833739 and grant VI 713/3-1, project no. 243500032). We acknowledge support by the Paderborn Center for Parallel Computing (PC2, HPC system Noctua 2) and by the Regional Computing Centre of the University of Cologne (RRZK, HPC system RAMSES) for providing computing time.

References

1 D. W. Stephan, G. C. Welch, R. R. S. Juan and J. D. Masuda, Reversible, Metal-Free Hydrogen Activation, *Science*, 2006, **314**, 1124–1126.
2 D. W. Stephan, Frustrated Lewis Pairs, *J. Am. Chem. Soc.*, 2015, **137**, 10018–10032.
3 D. W. Stephan, Frustrated Lewis Pairs: From Concept to Catalysis, *Acc. Chem. Res.*, 2015, **48**, 306–316.
4 A. R. Jupp and D. W. Stephan, New Directions for Frustrated Lewis Pair Chemistry, *Trends Chem.*, 2019, **1**, 35–48.
5 N. Li and W. Zhang, Frustrated Lewis Pairs: Discovery and Overviews in Catalysis, *Chin. J. Chem.*, 2020, **38**, 1360–1370.
6 R. F. Heck, Acylation, methylation, and carboxyalkylation of olefins by Group VIII metal derivatives, *J. Am. Chem. Soc.*, 1968, **90**, 5518–5526.
7 W. S. Knowles and M. J. Sabacky, Catalytic asymmetric hydrogenation employing a soluble, optically active, rhodium complex, *Chem. Commun.*, 1968, 1445.
8 R. H. Grubbs and T. K. Brunck, Possible intermediate in the tungsten-catalyzed olefin metathesis reaction, *J. Am. Chem. Soc.*, 1972, **94**, 2538–2540.
9 S. Baba and E. Negishi, A novel stereospecific alkenyl-alkenyl cross-coupling by a palladium- or nickel-catalyzed reaction of alkenylalanes with alkenyl halides, *J. Am. Chem. Soc.*, 1976, **98**, 6729–6731.
10 T. Katsuki and K. B. Sharpless, The first practical method for asymmetric epoxidation, *J. Am. Chem. Soc.*, 1980, **102**, 5974–5976.
11 N. Miyaura and A. Suzuki, Palladium-Catalyzed Cross-Coupling Reactions of Organoboron Compounds, *Chem. Rev.*, 1995, **95**, 2457–2483.
12 C. P. Johnston, R. T. Smith, S. Allmendinger and D. W. C. MacMillan, Metallaphotoredox-catalysed sp^3–sp^3 cross-coupling of carboxylic acids with alkyl halides, *Nature*, 2016, **536**, 322–325.
13 A. Y. Chan, I. B. Perry, N. B. Bissonnette, B. F. Buksh, G. A. Edwards, L. I. Frye, O. L. Garry, M. N. Lavagnino, B. X. Li, Y. Liang, E. Mao, A. Millet, J. V. Oakley, N. L. Reed, H. A. Sakai, C. P. Seath and D. W. C. MacMillan, Metallaphotoredox: The Merger of Photoredox and Transition Metal Catalysis, *Chem. Rev.*, 2022, **122**, 1485–1542.
14 J. Paradies, Mechanisms in Frustrated Lewis Pair-Catalyzed Reactions, *Eur. J. Org. Chem.*, 2019, 283–294.
15 R. Zhou, Z. P. Tavandashti and J. Paradies, Frustrated Lewis Pair Catalyzed Reactions, *SynOpen*, 2023, **7**, 46–57.
16 G. Ménard and D. W. Stephan, Room Temperature Reduction of CO_2 to Methanol by Al-Based Frustrated Lewis Pairs and Ammonia Borane, *J. Am. Chem. Soc.*, 2010, **132**, 1796–1797.
17 J. Chen, L. Falivene, L. Caporaso, L. Cavallo and E. Y.-X. Chen, Selective Reduction of CO_2 to CH_4 by Tandem Hydrosilylation with Mixed Al/B Catalysts, *J. Am. Chem. Soc.*, 2016, **138**, 5321–5333.
18 M. N. Khan, Y. Van Ingen, T. Boruah, A. McLauchlan, T. Wirth and R. L. Melen, Advances in CO_2 activation by frustrated Lewis pairs: from stoichiometric to catalytic reactions, *Chem. Sci.*, 2023, **14**, 13661–13695.
19 G.-Q. Chen, F. Türkyilmaz, C. G. Daniliuc, C. Bannwarth, S. Grimme, G. Kehr and G. Erker, Enamine/butadienylborane cycloaddition in the frustrated Lewis pair regime, *Org. Biomol. Chem.*, 2015, **13**, 10477–10486.
20 G. C. Welch and D. W. Stephan, Facile Heterolytic Cleavage of Dihydrogen by Phosphines and Boranes, *J. Am. Chem. Soc.*, 2007, **129**, 1880–1881.

21 C. M. Mömming, E. Otten, G. Kehr, R. Fröhlich, S. Grimme, D. W. Stephan and G. Erker, Reversible Metal-Free Carbon Dioxide Binding by Frustrated Lewis Pairs, *Angew. Chem., Int. Ed.*, 2009, **48**, 6643–6646.
22 E. Otten, R. C. Neu and D. W. Stephan, Complexation of Nitrous Oxide by Frustrated Lewis Pairs, *J. Am. Chem. Soc.*, 2009, **131**, 9918–9919.
23 D. W. Stephan and G. Erker, Frustrated Lewis pair chemistry of carbon, nitrogen and sulfur oxides, *Chem. Sci.*, 2014, **5**, 2625–2641.
24 Z. Mo, E. L. Kolychev, A. Rit, J. Campos, H. Niu and S. Aldridge, Facile Reversibility by Design: Tuning Small Molecule Capture and Activation by Single Component Frustrated Lewis Pairs, *J. Am. Chem. Soc.*, 2015, **137**, 12227–12230.
25 D. Zhu, Z.-W. Qu and D. W. Stephan, Addition reactions and diazomethane capture by the intramolecular P–O–B FLP: ^{t}Bu$_2$POBcat, *Dalton Trans.*, 2020, **49**, 901–910.
26 F. Breher, F. Krämer, J. Paradies and I. Fernández, A crystalline aluminium–carbon-based ambiphile capable of activation and catalytic transfer of ammonia in non-aqueous media, *Nat. Chem.*, 2024, **16**, 63–69.
27 M. Shang, X. Wang, S. M. Koo, J. Youn, J. Z. Chan, W. Yao, B. T. Hastings and M. Wasa, Frustrated Lewis Acid/Brønsted Base Catalysts for Direct Enantioselective α-Amination of Carbonyl Compounds, *J. Am. Chem. Soc.*, 2017, **139**, 95–98.
28 D. W. Stephan and G. Erker, Frustrated Lewis Pair Chemistry: Development and Perspectives, *Angew. Chem., Int. Ed.*, 2015, **54**, 6400–6441.
29 C. Appelt, H. Westenberg, F. Bertini, A. W. Ehlers, J. C. Slootweg, K. Lammertsma and W. Uhl, Geminal Phosphorus/Aluminum-Based Frustrated Lewis Pairs: C≡H versus C≡C Activation and CO_2 Fixation, *Angew. Chem., Int. Ed.*, 2011, **50**, 3925–3928.
30 R. G. Pearson, Hard and Soft Acids and Bases, *J. Am. Chem. Soc.*, 1963, **85**, 3533–3539.
31 H. Böhrer, N. Trapp, D. Himmel, M. Schleep and I. Krossing, From unsuccessful H_2-activation with FLPs containing B(Ohfip)$_3$ to a systematic evaluation of the Lewis acidity of 33 Lewis acids based on fluoride, chloride, hydride and methyl ion affinities, *Dalton Trans.*, 2015, **44**, 7489–7499.
32 J. Possart and W. Uhl, Influence of the Lewis Acidity of Gallium Atoms on the Reactivity of a Frustrated Lewis Pair: Experimental and Theoretical Studies, *Organometallics*, 2018, **37**, 1314–1323.
33 Y. Wang, Z. H. Li and H. Wang, Synthesis of an oxygen-linked germinal frustrated Lewis pair and its application in small molecule activation, *RSC Adv.*, 2018, **8**, 26271–26276.
34 J. Buth, Y. V. Vishnevskiy, J.-H. Lamm, B. Neumann, H.-G. Stammler and N. W. Mitzel, Tuning reactivity through implementation of the HSAB concept in oxygen- and sulphur-bridged Al/P and Ga/P FLPs, *Dalton Trans.*, 2026, **55**, 2691–2701.
35 L. Wickemeyer, N. Aders, A. Mix, B. Neumann, H.-G. Stammler, J. J. Cabrera-Trujillo, I. Fernández and N. W. Mitzel, Carbon dioxide reduction by an Al–O–P frustrated Lewis pair, *Chem. Sci.*, 2022, **13**, 8088–8094.
36 J. Buth, M. J. Klingsiek, Y. V. Vishnevskiy, A. Mix, J.-H. Lamm, B. Neumann, H.-G. Stammler and N. W. Mitzel, Aluminum versus Gallium: Differences in Bis(bis(trimethylsilyl)methyl) Element Halides, Hydrides, and Oxygen-Bridged E/P Frustrated Lewis Pairs, *ChemistryEurope*, 2026, **4**, e202500307.
37 L. Xing, W. Li, C. Wang, F. Gu, M. Xu, C. Tan and J. Yi, Theoretical Investigations on Oxidative Stability of Solvents and Oxidative Decomposition Mechanism of Ethylene Carbonate for Lithium Ion Battery Use, *J. Phys. Chem. B*, 2009, **113**, 16596–16602.
38 Z. Lu, Z. Li, J. Duan, X. Li, C. Liu and W. Xiao, Revisit coupling of CO_2 to ethylene carbonate with an integrated imidazolium and zinc halides catalyst by a study on its decomposition: Active center and mechanism, *Chem. Eng. J.*, 2024, **495**, 153687.
39 L. Wickemeyer, L. Hartmann, B. Neumann, H. Stammler and N. W. Mitzel, Differences in the Reactivity of Geminal Si–O–P and Al–O–P Frustrated Lewis Pairs, *Chem. – Eur. J.*, 2023, **29**, e202202842.
40 W. Uhl, H. R. Bock, M. Claesener, M. Layh, I. Tiesmeyer and E.-U. Würthwein, cis/trans Isomerism of Hydroalumination and Hydrogallation Products—Reflections on Stability and Rearrangement Mechanism, *Chem. – Eur. J.*, 2008, **14**, 11557–11564.
41 (*a*) CCDC 2528994: Experimental Crystal Structure Determination, 2026, DOI: **10.5517/ccdc.csd.cc2qwmgq**; (*b*) CCDC 2528995: Experimental Crystal Structure Determination, 2026, DOI: **10.5517/ccdc.csd.cc2qwmhr**; (*c*) CCDC 2528996: Experimental Crystal Structure Determination, 2026, DOI: **10.5517/ccdc.csd.cc2qwmjs**; (*d*) CCDC 2528997: Experimental Crystal Structure Determination, 2026, DOI: **10.5517/ccdc.csd.cc2qwmkt**; (*e*) CCDC 2528998: Experimental Crystal Structure Determination, 2026, DOI: **10.5517/ccdc.csd.cc2qwmlv**; (*f*) CCDC 2528999: Experimental Crystal Structure Determination, 2026, DOI: **10.5517/ccdc.csd.cc2qwmmw**; (*g*) CCDC 2529000: Experimental Crystal Structure Determination, 2026, DOI: **10.5517/ccdc.csd.cc2qwmnx**; (*h*) CCDC 2529001: Experimental Crystal Structure Determination, 2026, DOI: **10.5517/ccdc.csd.cc2qwmpy**.